Hindawi
Geofluids
Volume 2022, Article ID 4822714, 17 pages
https://doi.org/10.1155/2022/4822714

Research Article

The Identification and Reservoir Architecture Characterization of Wandering Braided River in Nanpu 1-29 Area, Bohai Bay Basin

Xueqian Pang,[1,2] **Cheng Xue**,[3] **Yangping Liu**,[3] **Li Yin**,[1,2] **Yufeng Gao**,[1,2] **and Yanshu Yin**[1,2]

[1]*School of Geosciences, Yangtze University, Hubei, Wuhan 430100, China*
[2]*Key Laboratory of Exploration Technologies for Oil and Gas Resources, Yangtze University, Ministry of Education, Wuhan 430100, China*
[3]*Exploration and Development Research Institute, Jidong Oilfield, PetroChina, Hebei, Tangshan 063200, China*

Correspondence should be addressed to Yanshu Yin; yys@yangtzeu.edu.cn

Received 8 March 2022; Revised 3 May 2022; Accepted 29 June 2022; Published 21 July 2022

Academic Editor: Yujie Yuan

Nanpu 1-29 Area of Jidong Oilfield in China is currently in the stage of high water cut and low recovery degree. The remaining oil development and adjustment are difficult because of the complex reservoir heterogeneity and the lack of analysis of the reservoir architecture due to the unclear river type. This study first used sedimentary background, granularity, core, and sand body distribution to determine the river type and believed it belongs to the wandering braided river. Combined with core and logging data, four types of sedimentary architectural elements were found in the study area, namely, channel bar, braided channel, floodplain, and basalt. Based on the scale measurement of many similar modern wandering braided rivers, core data, and empirical formulas, the scales of the braided rivers were determined. The quantitative relationships among the scale of the braided river, the channel bar, and the braided channel were established. With this constraint, the reservoir architecture was anatomized. The results showed two filling types of the braided channels, including sandy filling and muddy filling. The combination patterns of the channel bars and the braided channels could be divided into three types, namely, superimposed, standalone, and contact, and the contact type was the primary type. On the whole, it showed the geometric morphological characteristics of the flat top convex at the bottom of the channel bar and the flat bottom convex at the top of the braided river channel. A careful measure of the architectural element was executed. The length of the single braided flow belts was 365.16-1349.72 m, and the width was 270.57-1160.54 m. The channel bar's length was distributed 158.89-318.32 m, and the width was distributed 75.97-116.41 m. The braided river's width was distributed 16.81-180.05 m. The length and width ratio of the channel bar was concentrated between 2 and 4, which manifested wide bar and narrow river channel mode. Finally, the static distribution model and dynamic response curve were compared to verify the correctness of the reservoir architecture characteristics to guide the subsequent development of the oilfield.

1. Introduction

Reservoir architecture originated from the study of outcrops in ancient rivers. In 1977, Allen, the American scholar, first introduced the architectural term "Architecture" into the study of river reservoir sedimentation, which was used to describe the geometric form of the braided channel, overflow sedimentation, and their internal structure characteristics [1]. Under the influence of Allen's thought, Miall first proposed a complete analysis method of reservoir architecture elements of river facies [2], which defined the reservoir architecture as the geometry, size, direction, and interrelationship of reservoirs and their internal constituent units. Accordingly, the traditional meandering rivers and the braided rivers were subdivided. The braided rivers were divided into the sandy braided rivers and the gravel braided rivers. The sandy braided rivers included deeper and year-round sandy braided rivers, shallower and year-round sandy braided rivers, high-energy

sandy braided rivers, flood-end braided rivers, and other types [3]. Bridge and Tye used the ground penetrating radar technology to measure the scale of modern braided river sediments, and found that the shapes of the channel bar and the braided channel developed by braided river were very clear, and their thicknesses were similar [4]. Skelly et al. measured the sedimentary scale of the Niobrara River using ground penetrating radar, then found that the channel bars obviously could not be cut to the bottom by the braided channels, and their interfaces were poorly sharp and differed significantly [5]. Longxin and Guoliang and Dali et al. subdivided the sandy braided rivers into two categories based on the interpretation of the outcrop of the Datong braided river [6, 7], including branching type and wandering type. In her opinion, the branching type was a deeper water type with perennial flowing water, and the boundary between the channel bar and the river channel was clear. The wandering type was often unable to completely cut the channel bar due to the swing of the river, and the boundary between them was not noticeable. Controlled by the differences in their hydrodynamic environment and sedimentary environment, the developments of the muddy interlayers in the two different braided rivers were also various, resulting in apparent differences in sedimentary architecture and their control of oil-water distribution. In addition, the geometrical morphology of the channel developed in the deep water environment and the braided river is similar, but the sedimentary genesis of the two is quite different. The braided channel is traction flow deposition, while the deep water channel is gravity flow deposition. And during the development of deep water channel, sandbody complexes with different sizes and shapes are formed due to different degrees of vertical accretion and lateral migration [8, 9].

The primary layer of the study area is currently in the high water content stage, and the degree of production is low. However, geological studies have shown that the local remaining oil extraction has excellent potential. Therefore, it is urgent to carry out an architecture analysis to reveal the main controlling factors of the remaining oil distribution to provide a basis for oilfield development adjustment. In this paper, taking the Guantao Formation of Nanpu 1-29 Area as an example, the river type was determined based on sedimentary background, granularity, core, and sand body. On this basis, guided by the analytic hierarchy process, according to Miall's idea, the architecture research of the study area was carried out. Finally, the static distribution model and dynamic response curve of the study area were compared and analyzed to verify the correctness of the above reservoir architecture research and provide guidance for the subsequent development of the oilfield.

2. Overview of the Study Area

The Nanpu Depression is located in the northeast of North China and the southern edge of the Yanshan Terrace Fold Belt. It is a Meso-Cenozoic basin north of Huanghua Depression, Bohai Bay Basin. Drilling revealed the development of the strata from top to bottom in the area, including the Quaternary Plain Formation, the Upper Tertiary Minghuazhen Formation, the Guantao Formation, the Lower Tertiary Dongying Formation, the Shahejie Formation, the Mesozoic Cretaceous, Jurassic, and the Paleozoic Ordovician strata. The Guantao Formation is in integrated contact with the overlying Minghuazhen Formation, and the lower tertiary Dongying Formation is in nonintegrated touch. Nanpu 1-29 Area in this study belongs to the No. 1 tectonic belt of the Nanpu Depression. The main target area is the Neogene Guantao Formation, which is mainly developed braided river deposits with reservoir thickness of 300-900 m.

The drilling of the NP 1 well opened the prelude to exploring the Nanpu Oilfield on May 23, 2004. The primary layer is currently in the high water cut stage, and the degree of production is low. However, geological studies have shown that the local remaining oil still has excellent potential. Therefore, it is urgent to carry out an architecture analysis to reveal the main controlling factors of the remaining oil distribution and provide a basis for oilfield development adjustment.

3. Identification of River Type

Longxin and Guoliang established the distribution pattern of the reservoir architecture of the branching braided rivers and the wandering braided rivers [6], believing that the branching braided rivers had large curvature on the horizontal, and the main river was relatively stable. In the same period, the braided channel was significantly divided by the channel bar, the braided channel and the channel bar were superimposed laterally, and the thickness was very similar. In the end, the geometric form of the flat top convex at the bottom of the channel bar and the flat bottom convex at the top of the braided channel was presented. Some silting layers and chutes developed in the interior of the channel bars. There were many channels in wandering braided rivers, the curvature was slight, and the locations of the channel bars and the braided channels changed rapidly [10–13]. Due to the rapid change of the river, the sand body would produce the phenomenon of undercutting and overlapping during the movement. The positions of the braided channel and the channel bars were not fixed, and it was challenging to preserve the silting layer under the erosion of the strong water power of the river. In addition, based on the sedimentary background, it was found that there were still significant differences between the branching braided rivers and the wandering braided rivers in terms of production conditions due to the difference between the number of the braided channel, curvature, and width-to-depth ratio. In general, the wandering rivers were affected by floods, and the short-term outbreak of flooding caused siltation. Because the rivers were often diverted, the number of channels increased. While the water supply of the branching river was relatively stable, the growth of the channel bars and the braided channels was steady. So the diversion effect was weak, and the number of waterways was relatively stable. Based on four indicators, including sedimentary background, granularity characteristics, core characteristics, and sand body distribution, the river type was comprehensively judged to be a wandering braided river in the study area.

3.1. Sedimentary Background. Previous studies have shown that due to the abundant source of materials, large slopes, and rapid water flow, the Guantao Formation mainly developed alluvial

fan and braided river in the initial stage of sedimentation [14]. However, with the rise of the base level, the sedimentary slope decreased, and the river velocity slowed down gradually, leading to a gradual decrease in the scour effect, so the granularity of the sediments in the provenance became smaller, and the depression gradually disappeared. Intense tectonic activity played a favorable role in forming the alluvial fans and the braided rivers.

Based on the previous studies on paleoclimatic conditions of Nanpu Depression [15], it is found that the Guantao Formation has a variety of plant types, mainly including angiosperms such as ulmipollenites, momipites, and juglanspollenites; ferns such as ceratopteris thalictroides and filicinaes; and gymnosperms such as abietineaepollenites and pinuspollenites. All this indicated that the paleoclimate conditions during the sedimentation process of the Guantao Formation were scorching and arid. This scorching and dry paleoclimate condition provided the clastic materials needed for the formation of alluvial fans and braided rivers and facilitated the development of the wandering braided rivers.

3.2. Granularity Characteristics. The granularity curve showed that the study area was mainly characterized by steep two-segment curves (Figure 1). The rolling was not very well developed, primarily jumping and suspension. The φ values were concentrated primarily between 1 and 4, reflecting prominent fluvial facies granularity characteristics. According to the investigation of the modern Yongding River by Liao et al. [16], it was shown that there was a significant difference in the granularity curve of the braided river with a high slope and a low slope. In his opinion, the high slope braided rivers were mainly composed of three sections, and the proportions of rolling, jumping, and suspension were close to each other. The low-sloping braided rivers were dominated by two sections, and jumping occupied the main body. They also believed that it was possible to distinguish between low-slope and high-slope braided rivers according to the distribution of the granularity curve. Obviously, from the granularity curve characteristics, the braided river of the study area was closer to the low-slope type.

3.3. Core Characteristics. Different characteristics of granularity and bedding represent the variation of sedimentary hydrodynamic conditions, which plays a vital role in analyzing sedimentary genetic types and reservoir architecture [17]. According to the observation of the core wells, the lithology was mainly medium-coarse sandstone, with few fine-grained sedimentations and relatively few muddy interlayers in the sandstone (Figures 2 and 3). Thick muddy barriers were locally developed. Mudstone color was mainly brownish red, mixed with gray-green mudstone. Conglomerate could be seen locally. The gravel diameter was generally 2 cm. The directional column could be seen, and the roundness was general, reflecting the braided rivers' characteristics with near-source sedimentation.

There were abundant bedding structures and structural types, including scouring surface, massive bedding, large trough cross-bedding, parallel bedding, small cross-bedding, wave bedding, veined bedding, sand bedding, high/low angle cross-bedding, and deformation bedding (Figure 4). Massive bedding and trough cross-bedding were the main types. In contrast, the developments of high/low angle cross-bedding and tabular cross-bedding were limited in the study area, reflecting that the stable channel bar was not developed. However, mudstone interlayer was rarely observed in the core, indicating that the channel migration was rapid and the preservation degree of muddy sediment was low, consistent with the sedimentary characteristics of the wandering braided rivers.

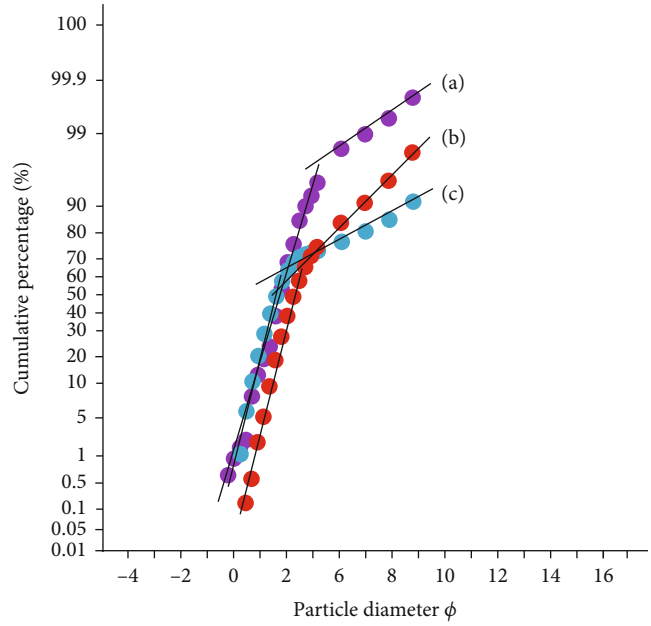

Figure 1: Granularity analysis of Nanpu 1-29 Area: (a) well NP12-86, 2773.07 m; (b) well NP12-43, 3014.13 m; (c) well NP12-X77, 2773.07 m.

3.4. Distribution Characteristics of Sand Body. There are significant distinctions in lithology, logging characteristics of different sand bodies, and the geometrical shape of sand bodies in horizontal and vertical [18–20]. According to the sand body thickness map (Figure 5), it is found that the sand body was generally distributed in concentrated and contiguous pieces, and mud sedimentation was less. In addition, the boundary of the sand body was relatively straight, with more minor bending characteristics and mat distribution characteristics. Because of the accretion and lateral accretion brought by paroxysmal floods, the distribution of the channel bar was connected and filled in the channel, which led to the braided channel deposition was not noticeable. The channel bars were gradually formed by the influence of the inertial centrifugal force of the river and the continuous accumulation of sediment in the flood period. Therefore, the formation of the channel bars was closely related to the braided channels. On the whole, the trough cross-bedding formed by the migration of the channel bar was the primary structural type.

In this paper, the sedimentary scale of the modern braided rivers, sand body thickness, and logging characteristics was combined to determine whether the channel bars and the braided channels were developed, and the sedimentary facies profiles were drawn in detail (Figure 6). The scales of the channel bars and the braided channels shown on the profile were in good agreement with the sedimentary scale of the modern

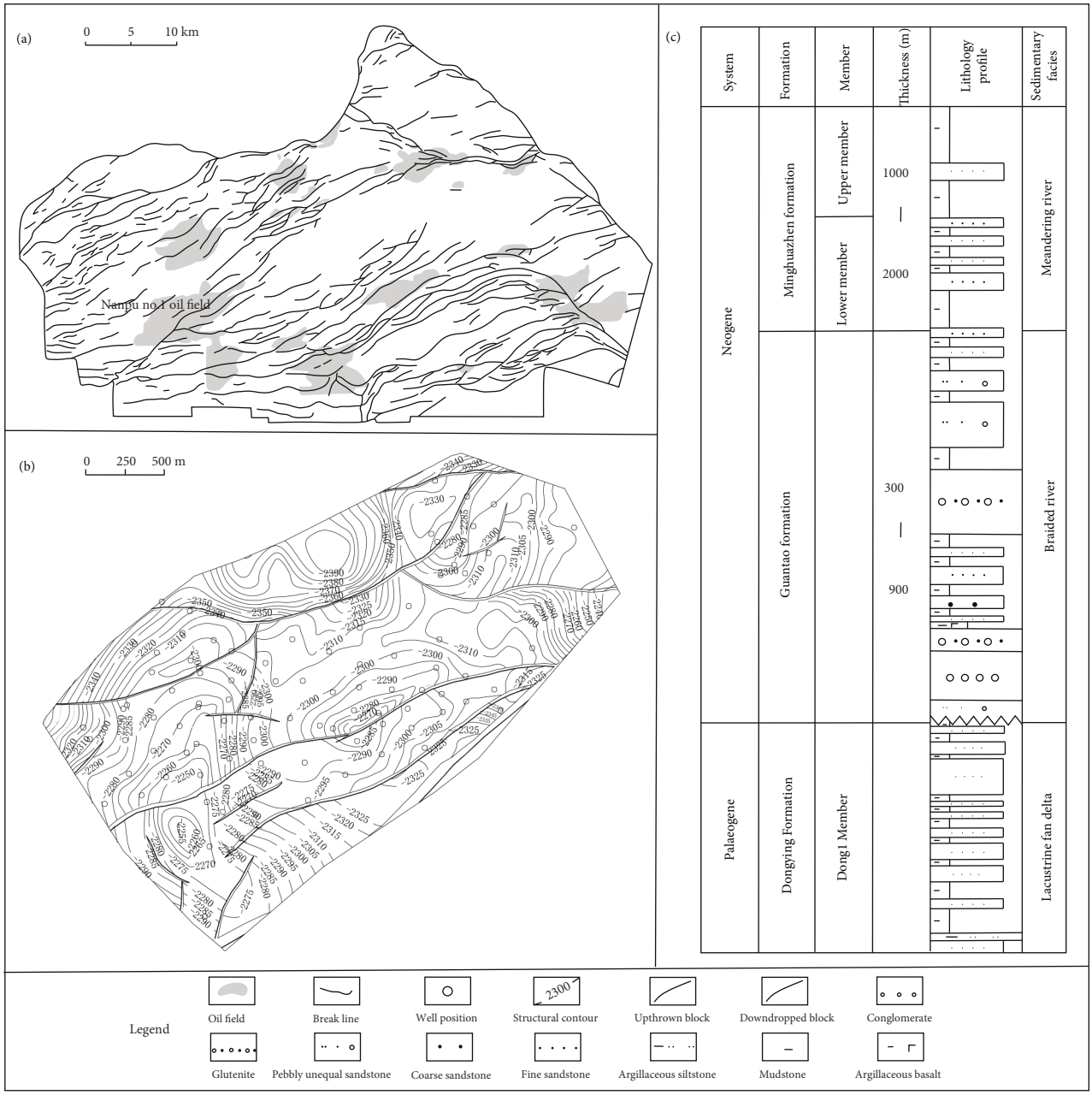

Figure 2: Structural location and comprehensive histogram of the study area: (a) structural location map of Nanpu Depression; (b) structural map of Nanpu 1-29 Area, located in Nanpu No. 1 oil field; (c) comprehensive histogram of Neogene in Nanpu Depression, the sedimentary sequences of a braided river and a meandering river were described.

braided rivers, which indicated that the sedimentary facies profiles were correct. In addition, the channel bars were relatively developed on the profile, interspersed with braided channels, and the proportion of latter development was relatively small. The thickness of the channel bar was slightly thicker than that of the braided channel, and the channel would not completely cut the channel bar. A small number of muddy interlayers were developed in the sand body, but very little was developed in the channel bar, and only the scour surface was retained, indicating that the river had strong hydrodynamic force and high sedimentary energy, so it was difficult to form the muddy interlayer. On the whole, it showed the geometric morphological characteristics of the flat top convex at the bottom of the channel bar and the flat bottom convex at the top of the braided channel, which was manifested in the style of wide bar and narrow braided channel.

3.5. Identification of River Type. Based on four indicators that are sedimentary background, granularity characteristics, core characteristics, and sand body distribution, the river

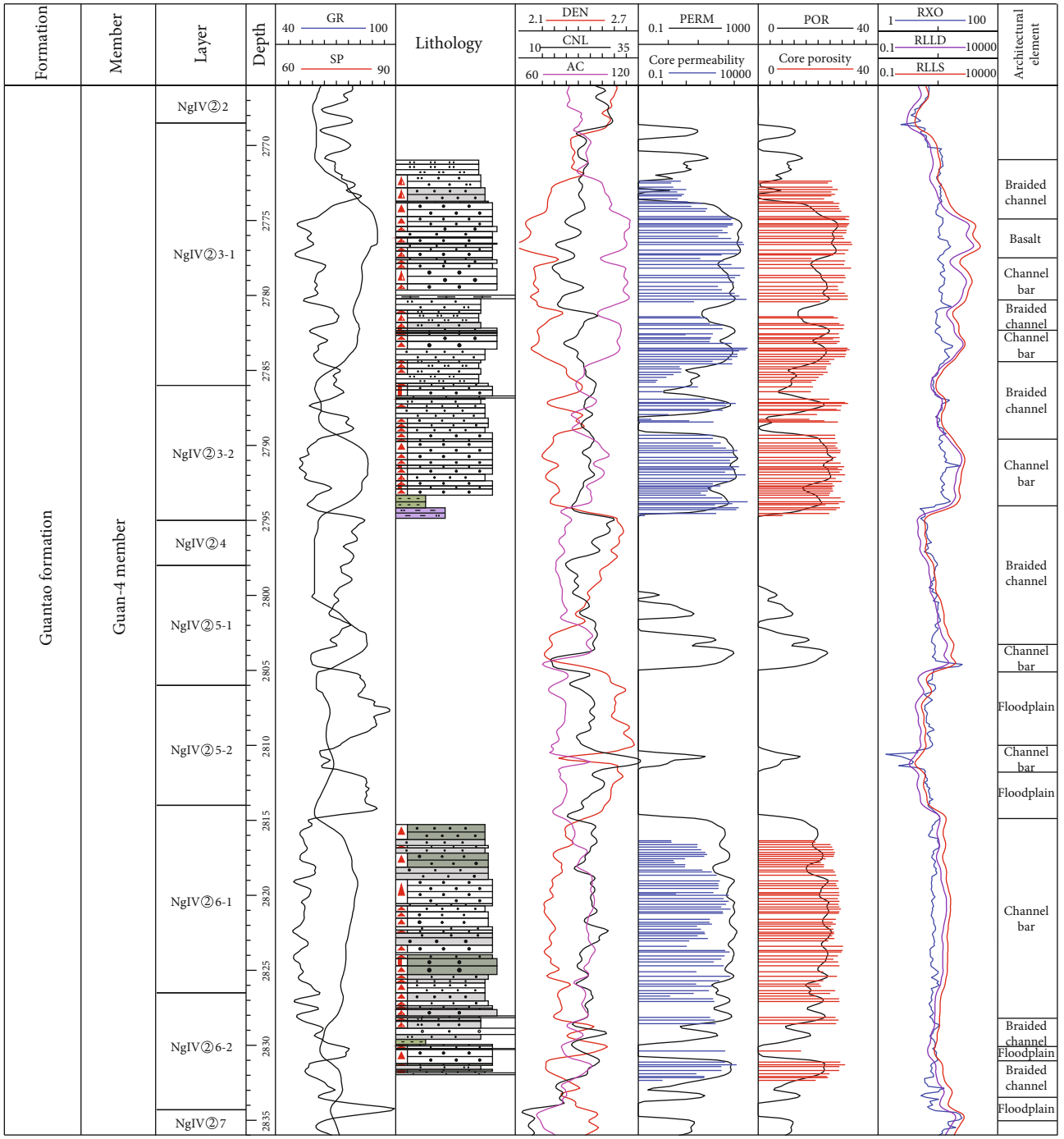

Figure 3: Comprehensive histogram of well NP12-X77 in Nanpu 1-29 Area.

type is comprehensively judged to be the wandering braided river in the study area. The specific reasons are as follows.

Firstly, the Guantao Formation of Nanpu 1-29 Area is in the late stage of structural depression, and the slope is relatively small on the whole.

Second, the braided rivers in the study area are close to the provenance area, and the hot and dry paleoclimate conditions will intensify the weathering. In this case, the seasonal flood events will lead to the scouring and silting of the river channel, and the river will be wandering on the horizontal.

Thirdly, according to the characteristics of bedding structure, it is found that trough bedding and massive bedding are primarily developed. In contrast, tabular cross-bedding with high/low angle is less developed, which indicates that the channel flow direction is easy to change, the deposition location of the channel bar is not fixed, and braided channel and channel bar cut and eroded each other.

Fourthly, combined with the contour map of sand body thickness, it is found that most of the sand bodies in Nanpu 1-29 Area present mat distribution with a low bending degree,

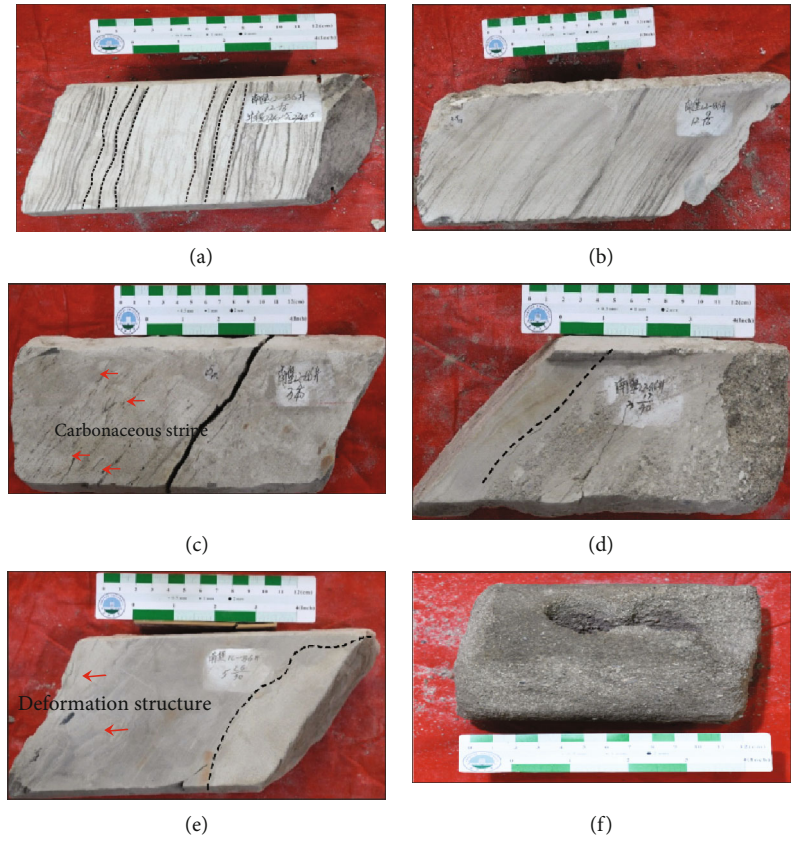

Figure 4: Sedimentary tectonic features of Nanpu 1-29 Area. (a) Wavy bedding, the bedding units that are symmetrical or asymmetrical wavy. (b) Ripple lamination fine sandstones, whose composition, color, and grain size change along the direction of sediment accumulation. (c) Veined carbonaceous fine sandstone, the sandstone is relatively sufficient, and there are abundant carbonaceous strips. (d) Massive bedding fine conglomerate, developed at the bottom of a river with a scour surface visible. (e) Sandy mass, which belongs to abnormal predrainage deposition, with deformation structure visible. (f) Massive bedded coarse sandstone, formed by rapid fluvial deposition.

less development of muddy interlayer on the profile, and width to depth ratio of more than 100.

In conclusion, the braided river type is determined to be the wandering braided river.

4. Characteristics of Sedimentary Architectural Elements

According to the core and logging curve data in the study area, it was found that the braided rivers in Nanpu 1-29 Area mainly developed four types of sedimentary architectural elements, namely, channel bar, braided channel, floodplain, and basalt (Figure 3). The logging characteristics of different sedimentary architectural elements were quite different [21].

4.1. Channel Bar. Channel bar is the main sedimentary architectural element of the braided rivers, with large sand thickness and a wide distribution range. The downstream accumulation of sediments forms the channel bar. The lithology is dominated by medium-fine sandstone as cemented fine sand, with uniform granularity and large sand body thickness. The logging curve presents a medium-high amplitude microdentate box shape, bell-shaped, and box-shaped form. These characteristics can be used as the basis to determine the channel bar. The erosion surface could be visible at the bottom, and pebbled sandstones are locally developed. The sedimentary structure is dominated by the trough cross-bedding and the low-angle cross-bedding.

4.2. Braided Channel. Like the channel bar, the braided channel is also the main sedimentary architectural element of the braided river, which is widely distributed in the study area. The braided channel is characterized by medium and low microtoothed bell shape, abrupt change at the bottom and gradual change at the top. The lithology is dominated by medium-fine sandstone. All these can be used as the basis for judging the braided channels. Compared with the channel bar of the same period, the sand body thickness is slightly smaller, reflecting cross-bedding and parallel bedding under strong hydrodynamic conditions.

According to the difference between filling lithofacies and filling thickness, it is found that there were two types of filling for the braided channel's development in the study area, namely, sandstone filling and mudstone filling. The braided channel of sandstone filling referred to the braided channel where sandstone filling sediment was the main part [22]. Due to the low flow rate and the low load capacity of the river, the sediment carried by the river was deposited, thus forming the sandstone filling channel, which presented a lenticular shape with a top flat and a convex bottom on the

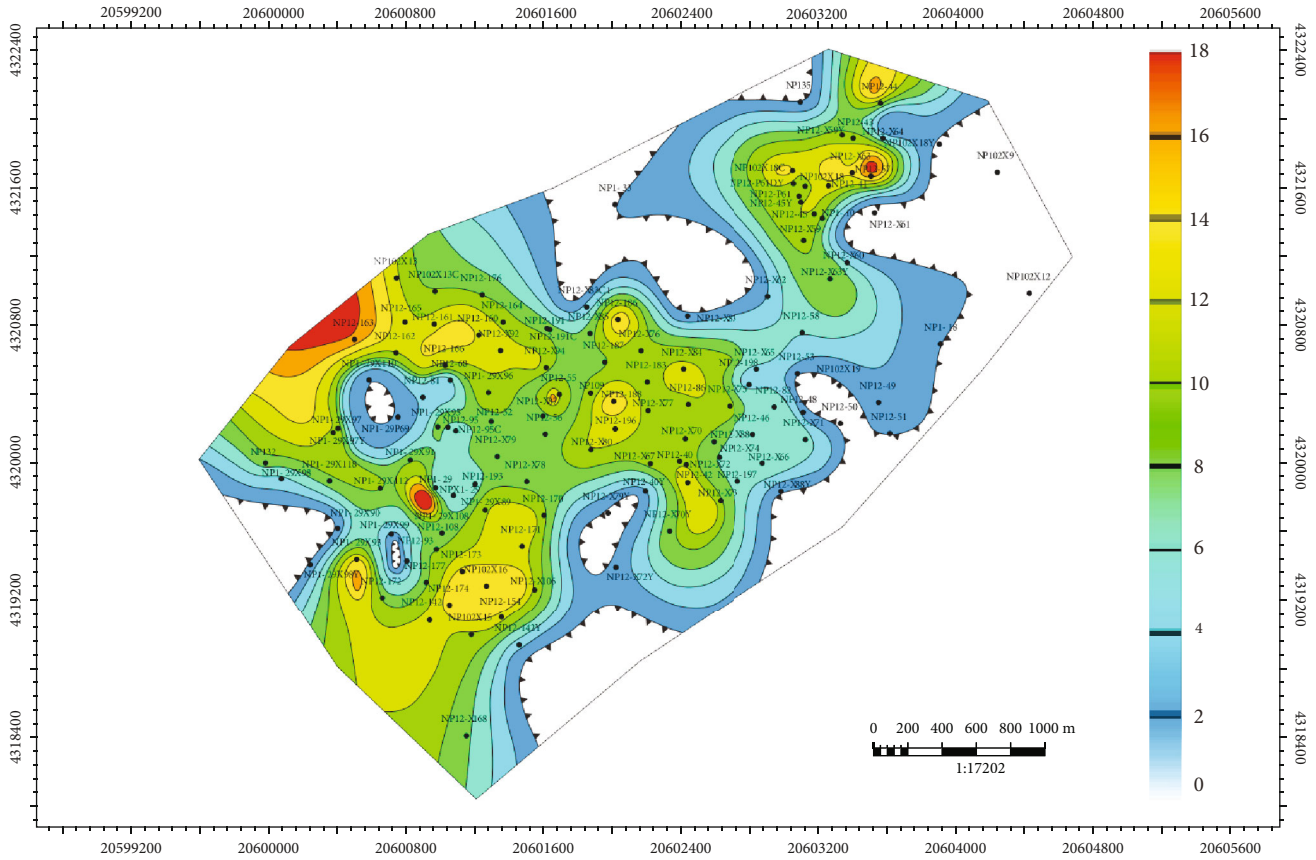

Figure 5: Contour map of NgIV②6-1 sand thickness in Nanpu 1-29 Area.

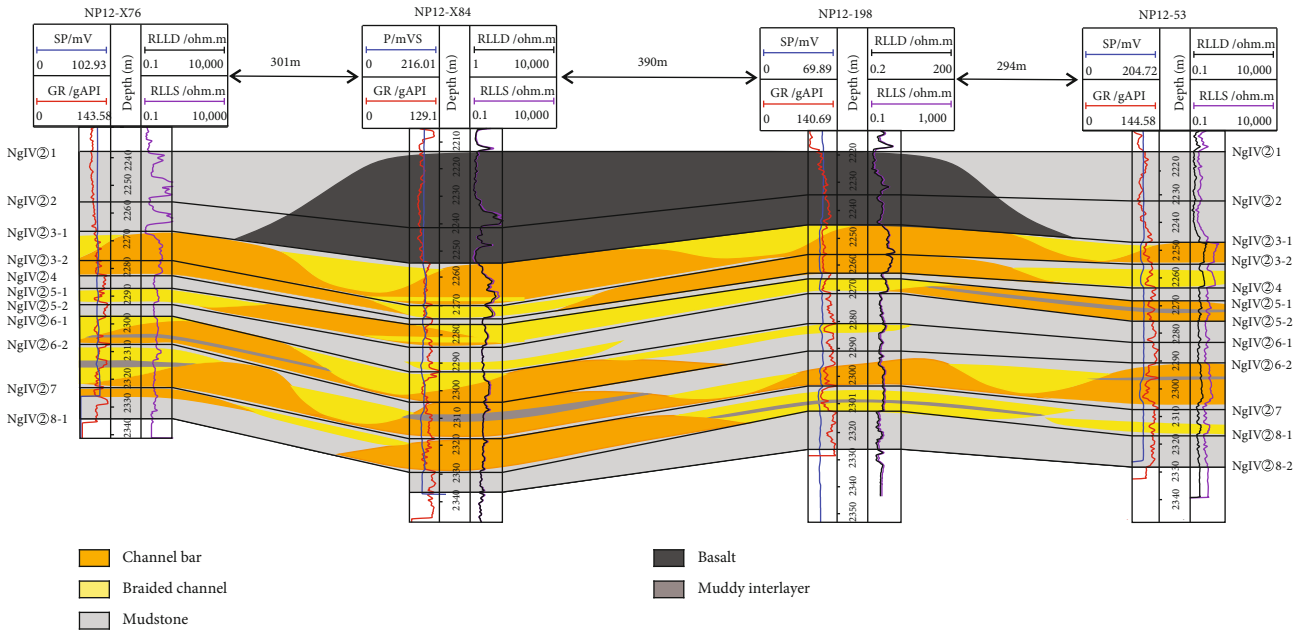

Figure 6: The vertical profile of sedimentary facies in Nanpu 1-29 Area. The study area and the scale of modern typical wandering braided river deposits and the scales of sedimentary architectural elements were determined.

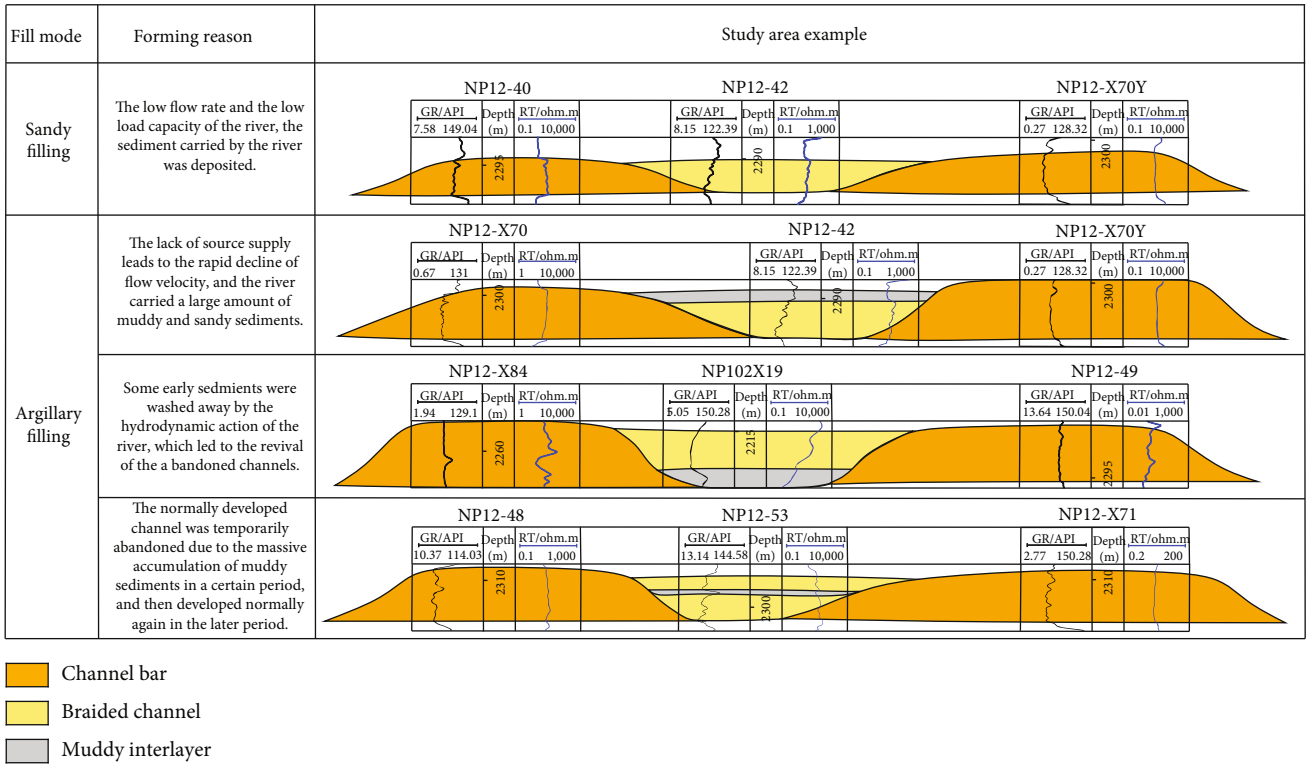

Figure 7: Filling pattern of the braided river in the study area.

profile. The braided channel mudstone filling was manifested in three [23] (Figure 7). The first was a form referring to the sandstone sediments filling in the bottom of the river channel and the mudstone sediments filling in the upper of the river channel. The reason for this phenomenon was that the lack of source supply led to the rapid decline of flow velocity, and the river carried a large amount of muddy and sandy sediments, which eventually led to the braided channel presenting a state of mudstone in the upper part and sandstone in the lower part. The second was the muddy sediments filling in the bottom of the river channel and the sandstone sediments filling in the upper of the river channel. This phenomenon occurred because some early sediments were washed away by the hydrodynamic action of the river, which led to the revival of the abandoned channels, thus forming the state of mudstone in the bottom part of the channel and sandstone in the upper part. The third was that the muddy sediments filling in the middle of the sandy river channel; that was, the normally developed channel was temporarily abandoned due to the massive accumulation of muddy sediments in a certain period and then developed normally again in the later period.

4.3. Floodplain. The floodplain is mainly developed on both sides of the braid flow belt, the lithology is dominated by massive mudstone and muddy siltstone, and the color is predominantly brown and dark brown, with no apparent bedding. The effective sand body thickness is thin, and the logging curve shows the linear characteristics with low amplitude microtoothed.

4.4. Basalt. There is also a special lithology affected by the volcanic eruption, namely, basalt, a kind of dense rock formed after the condensation of volcanic eruption magma. The lithology is dominated by basaltic mudstone, and the GR curve and SP curve on the logging curve are displayed as low values, showing a box-shaped form.

5. Classification and Quantitative Characterization of Reservoir Architectures

5.1. Classification of Reservoir Architecture. According to Miall's reservoir architecture classification scheme, the reservoir architecture interface of the study area was divided into 5-3 levels by using the hierarchical analysis method. The fifth level interface was a single braided flow belt, which belonged to the river channel filling unit. The fourth level interface was the sedimentary architectural element, where the single braided flow belt was mainly refined into the channel bars and the braided channels. The third level interface was the inner muddy interlayer level of the channel bar, with a thickness of about 1 to 2 cm.

Due to the thin thickness and difficulty preserving muddy interlayer, it was more difficult to track between wells accurately. In contrast, the braided flow belt was more accessible to identify than the muddy interlayer. Therefore, this study focused on the single braided flow belt, channel bars, and braided channels within the single flow belt. We first investigated the scale information of the modern braided rivers to

Table 1: Scale measurement results of typical wandering braided. All data are based on measurements taken on Google Earth.

River name	Channel bar width/m	Channel bar length/m	Braided channel width/m	Distance from the source area	Plains/ mountains
Thjorsa River	29.80	128.97	16.25	Distant source	Plain
Torrente Ferro River	30.38	139.14	10.84	Near source	Plain
Huseyjarkvisl River	61.77	152.97	17.67	Distant source	Plain
Rakaia River	157.68	534.82	25.56	Near source	Plain
Waimakari River	128.38	365.95	41.53	Near source	Plain
The front section of the Markham River	92.43	383.06	18.80	Near source	Plain
Buha River	56.45	220.80	14.05	Distant source	Plain
New Zealand River	61.69	155.81	22.04	Distant source	Plain
Godley River	66.90	253.96	11.42	Distant source	Mountain area
Rakaia River	265.52	747.40	89.22	Distant source	Mountain area
Lhasa River	124.48	356.52	28.08	Near source	Mountain area

get the quantitative relations of the reservoir architectural elements, to guide the anatomization of the subsurface reservoir.

5.2. Scale Investigation of Braided River Sedimentation. It is necessary to estimate the scale of the braided river for boundary identification to guide oilfield reservoir anatomy. Previous studies have determined the relationship among the cross strata, paleowater depth, and paleochannel based on many modern sediment and ancient outcrop analyses. The scale of the braided rivers in Nanpu 1-29 Area is predicted based on the scale of interbedded strata based on core statistics. The core statistics show that the average thickness of the cross strata in the study area was 0.3 cm.

The formula for estimating the thickness of a dune based on Leclair and Bridge [24] is

$$H = (2.9 \pm 0.7)h, \tag{1}$$

where H represents the dune's height and h represents the average thickness of the staggered stratigraphy.

According to the formula provided by Allen (1970), the relationship between the height of dunes and the paleowater depth is determined as follows:

$$d = 11.6 \times H^{0.84}, \tag{2}$$

where d is the water depth of the paleochannel.

The relationship between the water depth of the average paleochannel and paleochannel is as follows:

$$d_m = \frac{d}{2}, \tag{3}$$

where d_m is the average paleochannel water depth; the depth distribution range of paleochannel is strongly compared with previous studies [25].

The formula for predicting the braided channel's width according to Bridge and Tye [4], after the paleochannel depth is obtained, the width of the braided flow belt could be predicted:

$$Ch_w = 59.9d_m^{1.8}, \tag{4}$$

where Ch_w represents the braided channel's width.

According to the above formulas, the predicted water depth of the study area was 4.43-6.7 m, the thickness of the statistical channel bar was 1.8-5.92 m, and the width of the braided river was 872-1838 m.

On this basis, the sedimentary scale of 11 wandering braided rivers similar to the braided river in the study area was measured based on Google Earth [26] (Table 1), and the quantitative relationships between the channel bar's length and the channel bar' s width, as well as between the width of channel bars and the width of the braided channels, were determined (Figure 8). These quantitative relationships could be used to delineate the boundary between braided flow belts, braided channels, and channel bars.

5.3. Characteristics of Reservoir Architecture

5.3.1. Characteristics of Level 5 Reservoir Architecture. Reservoir architecture of level 5 in the study area refers to the single braided flow belt, and the identification of the single braided flow belt can provide a rich geological basis for determining the injection of oil and water and the direction of water flow, the connectivity between sand body, and the direction of channel extension. The identification methods of the single braided flow belt are as follows.

First is the method of sand body thickness analysis. The overall sedimentation of the braided river is characterized by the thicker inner center and the slightly thinner wings of the braided river belt; the channel top surface of the same river is isochronously deposited, and the braided flow belts of different periods within the same single layer will cause local sedimentation due to rapid migration and change. Therefore, the interfluvial sand body with the discontinuous distribution

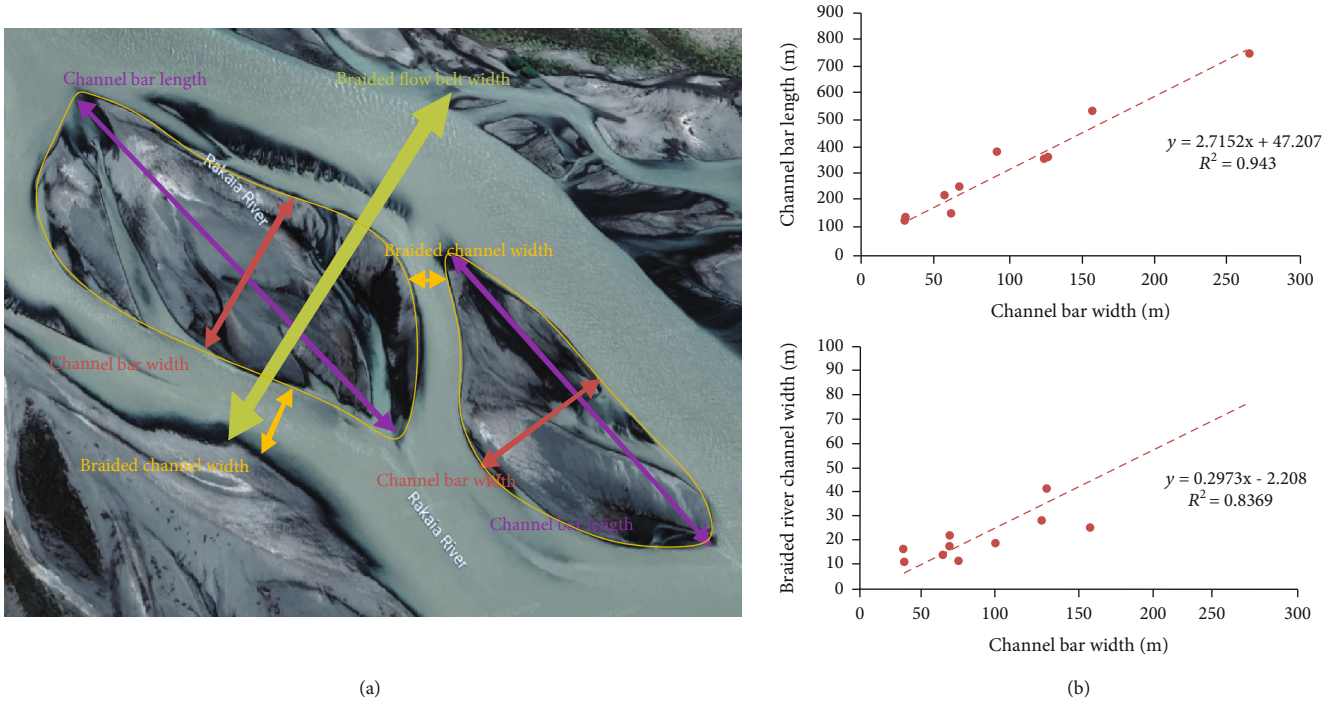

(a) (b)

Figure 8: Sedimentary scale of the modern typical wandering braided rivers. (a) The demonstration measurements of the channel bars, the braided channels, and a single braided flow belt based on Google Earth, taking the Rakaia River for example. (b) The relationships between the channel bar's length and the channel bar's width and between the channel bar's width and the braided channel's width based on the result data.

can be used as one of the markers for demarcating the boundary of the braided flow belt. Second is the floodplains between the braided flow belts. During the flood period, the sediments carried by the river are easy to deposit and form the floodplains, which can be used to judge the boundary of the braided flow belt. Finally, it can be judged by the top elevation difference of the sand body. During the flood period, the river level is higher than that of the channel bar, and the channel bar is exposed to the water surface during the dry period. The rapid change of the braided channels leads to the river sand gradually undercut and overlapping in continuous erosion. Due to the significant difference in the sedimentary environment required by the development of the sand body at different periods [27], the elevation difference of the top surface of the braided channel sand body might be quite different, which could be used as an identification mark of the sand body boundary.

This study fully referred to the scale of modern braided river deposition, combined with the empirical formula and the braided flow belt identification mark, to complete the horizontal map of sedimentary facies. The study found that the length and width of the single braided flow belt in the study area were 365.16-1349.72 m and 270.57-1160.54 m, which was consistent with previous studies and modern braided river deposition, indicating the correctness of the sedimentary facies map in the study area.

5.3.2. Characteristics of Level 4 Reservoir Architecture. Reservoir architecture of level 4 refers to the spread study of the channel bar and the braided channel inside the single braided flow belt, which is the premise of studying the muddy interlayer inside the sand body.

The change of thickness and width in the sand body is obviously due to the frequent swing of the channel. Sand body superposition relationship is a comprehensive reflection of hydrodynamic conditions, sediment supply efficiency, channel changes, and vertical evolution of sedimentary facies [28]. Many previous studies have been carried out on the superimposed shape and contact relationship of sand bodies. Although there are significant differences, the formation mechanism is relatively similar. Based on previous research results, Guo et al. made a comprehensive analysis of core data, logging data, sand body morphology, and sand body thickness and finally divided the superimposition types of sand bodies in southeastern Sulige into four types, including massive sand bodies, multilayered sand bodies, sectional interbedded sand bodies, and thin interbedded sand bodies [29].

Based on the characteristics study of single well facies and sedimentary architectural elements, it is found that the combination modes of the channel bars and the braided channels could be divided into three types, namely, superposed, standalone, and contact (Figure 9), and the contact type is the main type. The superposed mode refers to the fact that the single sand body developed in different periods has certain contact or no contact vertically, and the single sand body formed in the late period has no strong erosion and scouring effect on the single sand body formed in the early period [30]. The independent type refers to the pattern in which the single sand bodies developed at different times

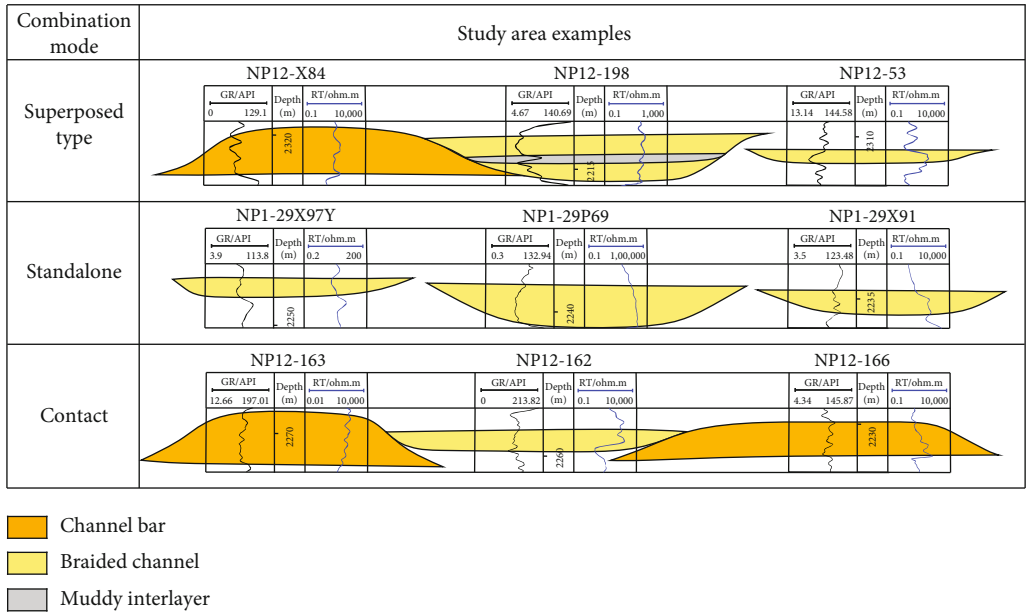

Figure 9: Combination pattern of the sand body in Nanpu 1-29 Area. The determination of the channel bar and the braided channel is mainly based on logging curve morphology and sand body thickness. The scale of channel bar and braided channel was obtained by referring to the scale of modern typical wandering braided river deposits, empirical formula, cores, and logging data in the study area.

are separated by some muddy sediments and do not contact each other [31]. The contact type refers to the vertical contact between the two periods of a single sand body, and the single sand body formed in the later period has some certain erosion and scouring effect on the single sand body formed in the earlier period. According to the above observations, the combination modes between the braided channels and the channel bars were more familiar.

Different overlapping styles of the sand body have different effects on development. The core data shows that each single sand body has different reservoir property characteristics, which indicates that each single sand body has a strong heterogeneity. Injected water will preferentially enter the areas with good physical properties and high permeability, and the areas with poor physical properties and low permeability will have less impact. Therefore, given this situation, the development of the remaining oil should focus on the physical properties and permeability parameters of the study area.

It is observed that there were more stable small layers in the study area, most of which were independent lenticular single sand bodies with great differences in thickness and shape. At this time, the effect could only be one-way. By contrast, the oil layer, closing to the injection well, had a faster flooding speed. This resulted in the good side of enrichment of remaining oil being more relative to the other side of the situation. In this case, the remaining oil development needed to pay more attention to the degree of water flooding by wells.

Combined with the characteristics of core, logging curve, sand body thickness, top surface elevation difference, and sedimentary facies transition, it is found that the combination mode between the channel bars and the braided channels was more contact type. The composite arc rhythms between the contacting composite sand bodies were obvious, and the heterogeneity was very strong, which led to the inconsistency of water displacement degree in each part and the formation of remaining oil. Therefore, it is necessary to pay attention to the uneven degree of water flooding for each oil layer in the process of remaining oil development.

In this study, the scale of modern typical wandering braided river deposition was measured based on Google Earth; thus, a quantitative reference was obtained for the actual drawing of sedimentary facies horizontal map and vertical profile. At the same time, combined with the characteristics of the logging curve and sand body thickness, the sedimentary scales of the channel bars and the braided channels could be identified and determined. The results were in good agreement with the scale of modern braided river deposition, indicating that the mapping results were accurate. Taking NgIV②6-1 as an example (Figure 10), it is observed that the maximum length of the channel bar was 318.32 m, the minimum was 158.89 m, and the average was 208.72 m. The maximum width of the channel bar was 116.41 m, the minimum was 75.97 m, and the average was 91.27 m. The maximum width of the braided channel was 180.05 m, the minimum was 16.81 m, and the average was 35.67 m. The anatomy reproduced well the distribution and scale characteristics of the channel bar and the river channel.

Dissecting each small layer of the study area and calculating its size (Table 2 and Figure 11), it showed that the length of a single channel bar was about 158.89-318.32 m, with an average of 209 m, and the width of a single channel bar was 75.97-116.41 m, with an average of 91 m. The width of the braided channel was about 16.81 m-180.05 m, with an average of 36 m. Meanwhile, the ratio of length and width for the channel bar was concentrated between 2 and 4.

In the horizontal map, the determination of which wells were distributed in the same channel bar was mainly based on the logging curve morphology and sand body thickness. If the logging curve morphology of several wells was all shown

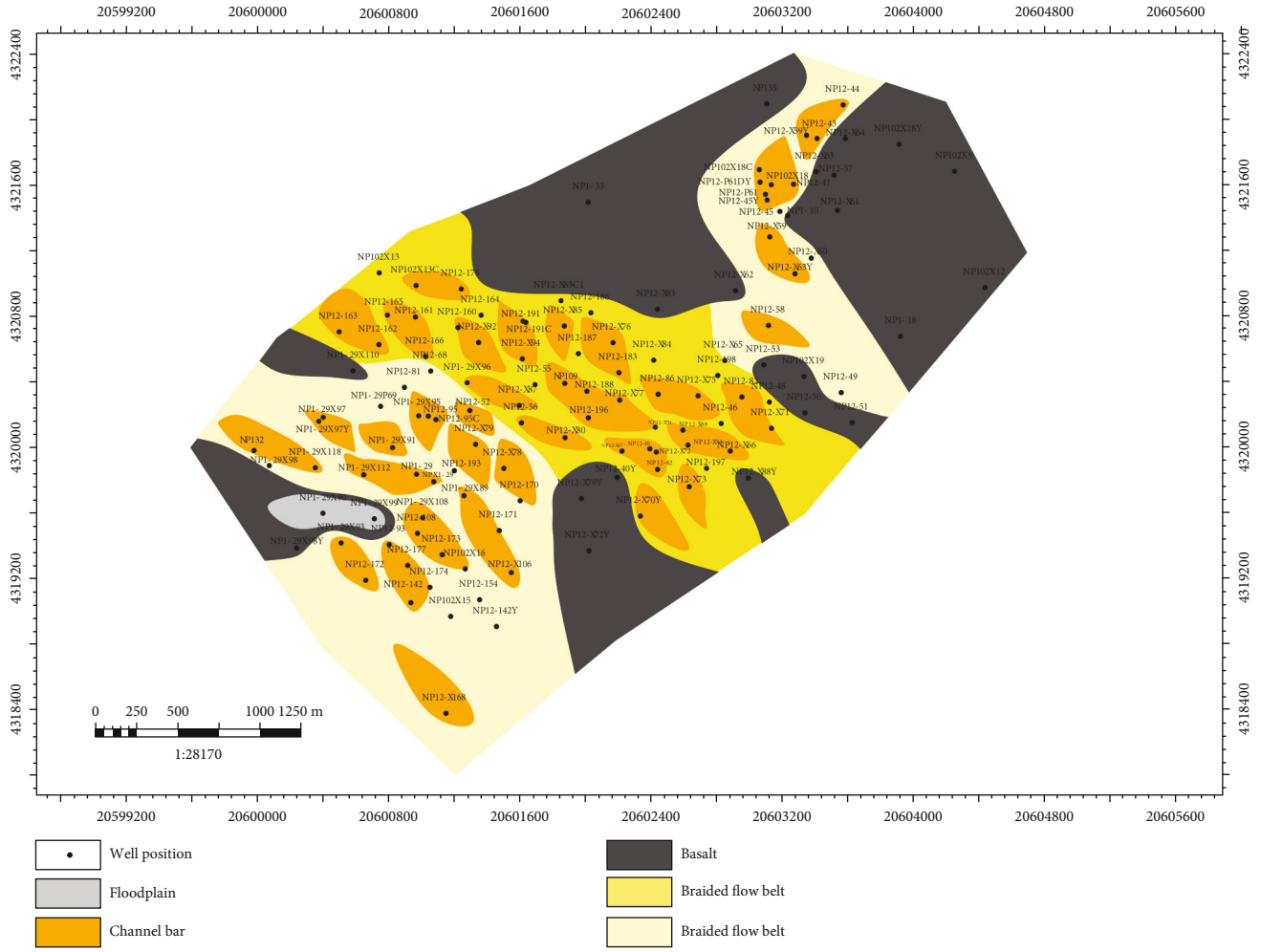

Figure 10: Sedimentary facies horizontal map of NgIV②6-1 in Nanpu 1-29 Area. The scale of the sedimentary architectural elements was obtained by referring to the scale of modern typical wandering braided river deposits, core data, and logging data in the study area. Different colors were used here to help distinguish the braid flow belt.

Table 2: Table of scale quantitative statistics between the channel bars and the braided channels in Nanpu 1-29 Area.

The layer number	Channel bar length/m			Channel bar width			Braided channel width		
	Maximum	Minimum	Average	Maximum	Minimum	Average	Maximum	Minimum	Average
3-1	188.69	177.00	183.00	86.59	75.97	81.00	23.51	18.62	21.00
3-2	242.35	232.10	237.00	99.23	84.65	92.00	30.33	21.12	26.00
5-1	200.60	158.89	185.00	87.22	81.25	85.00	61.93	18.34	40.00
5-2	204.43	158.91	181.00	93.71	78.07	83.00	180.05	20.12	75.00
6-1	207.23	175.84	193.00	95.53	84.23	91.00	48.78	18.42	30.00
6-2	247.97	213.46	231.00	114.00	98.90	106.00	23.60	19.93	22.00
7	211.85	206.37	208.00	101.85	96.25	98.00	31.18	21.60	25.00
8-1	219.93	205.23	213.00	89.86	87.08	88.00	29.69	16.81	23.00
8-2	318.32	289.52	304.00	116.41	90.25	103.00	35.68	34.10	35.00

as channel bar and the sand body thickness was relatively similar, these wells were judged to be in the same channel bar. If only one well was distributed or the other wells were distributed far away and the log showed medium-high amplitude microtooth box, bell-box, and thick sand, the channel bar was controlled by only one well.

5.3.3. Characteristics of Level 3 Reservoir Architecture. The result of core observation showed that there was a small number of muddy interlayer sediments in the channel bars [32] (Figure 12), which represented the migration of the bottom type caused by small floods. Affected by channel oscillation, these muddy interlayers were often difficult to preserve due

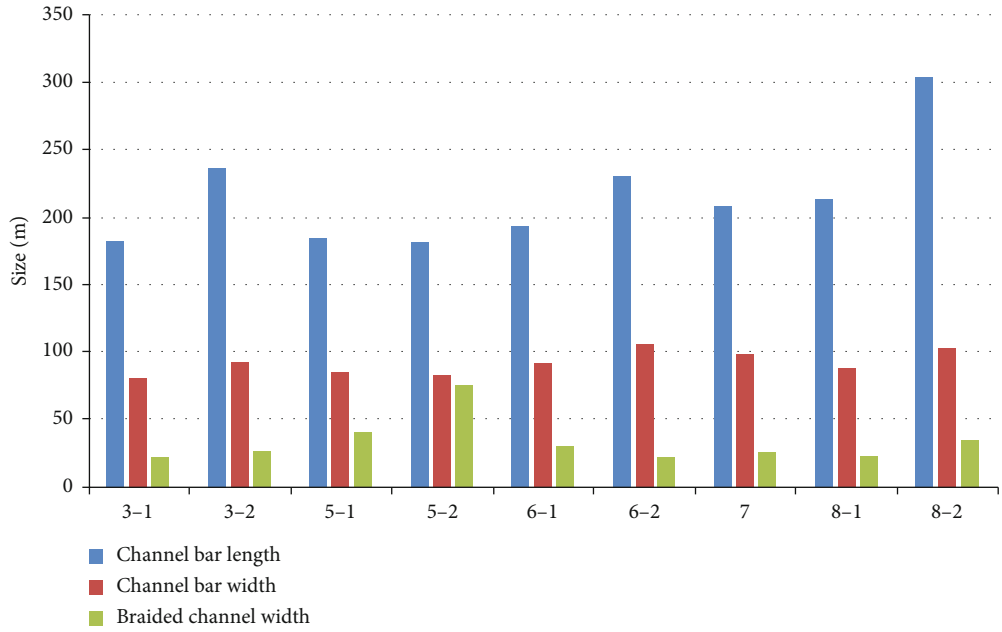

Figure 11: Quantitative statistical histogram of Nanpu 1-29 Area.

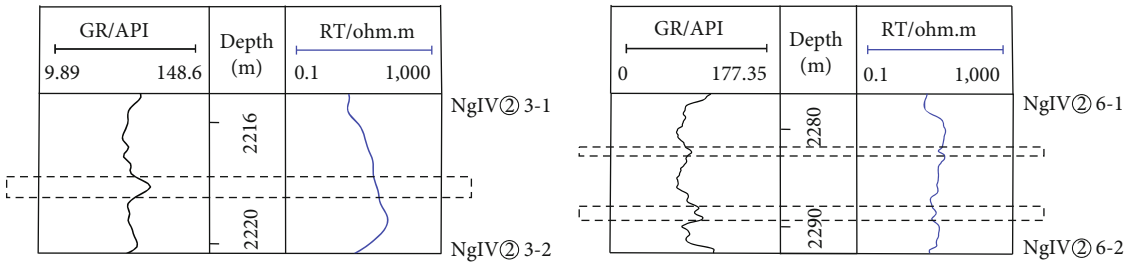

(a) NP1-29X99 (b) NP12-44

Figure 12: Identification mark of muddy interlayer in Nanpu 1-29 Area.

to extreme erosion, primarily manifested as fine-grained muddy interlayers inside the channel bars, mainly identified by the local return of the core and logging curve. Combined with the development process of the channel bars, considering the influence of water erosion and river accretion, the development scope and characteristics of the muddy interlayers inside the channel bars were studied, and the thickness of these muddy interlayers was about 1 to 2 cm.

6. Dynamic Data Verification

The dynamic development data of the oil field can be used as a verification of the reservoir architecture work [33], including the oil production, liquid production, and comprehensive water cut of the production wells and injection volume of the injection wells. For example, after water is injected into the reservoir from the injection wells, the crude oil will flow to the production wells in the direction of better connectivity and then be produced from the production wells. The fluctuation of the fluid production in the production wells is closely related to the connectivity of the injection wells. Generally, the better the connectivity, the more pronounced the correlation between the injection volume of the injection wells and the fluctuation amplitude of the liquid production volume in the production wells. Conversely, the poorer the connectivity, the smaller the correlation. Therefore, the static distribution model and dynamic response curve of the study area were compared and analyzed based on the dynamic development data to verify the correctness of the reservoir architecture research.

Four production wells named well NP12-172, well NP12-173, well NP12-142, and well NP12-174 and one injection well named well NP12-177 were selected, and the injection well was taken as the center of the well group. A static distribution model (Figures 13 and 14) was established based on the reservoir architecture interface of the 5-3 stage to analyze the dynamic connectivity between the two wells. By observing the static distribution model of the NP12-177 well group, it is found that the connectivity was good because the sand bodies between the well NP12-177 and well NP12-173 were mostly developed, while the development degree of muddy interlayer

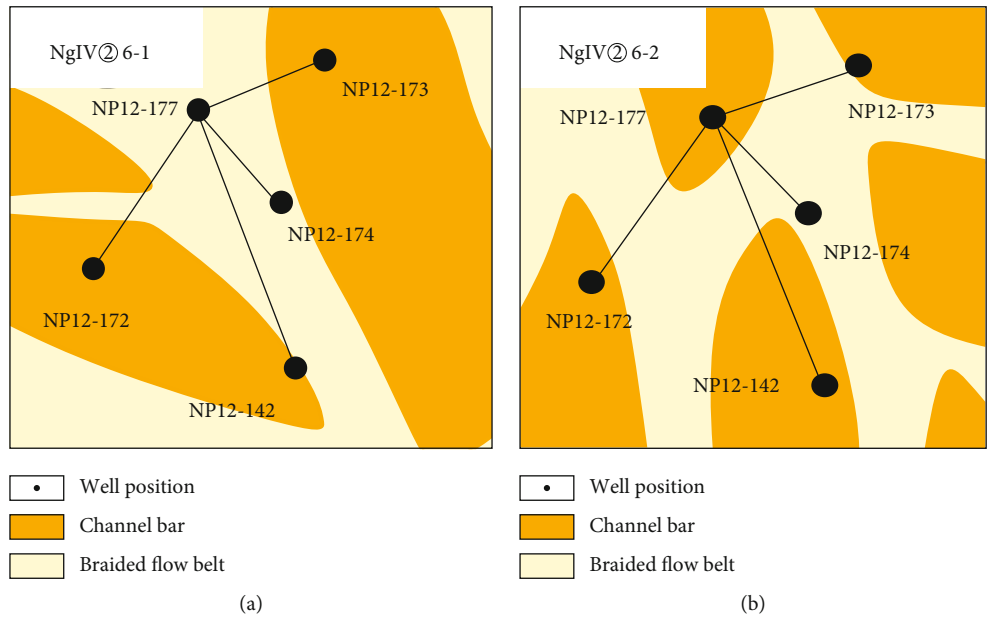

Figure 13: Perforating interval map of well group NP12-177.

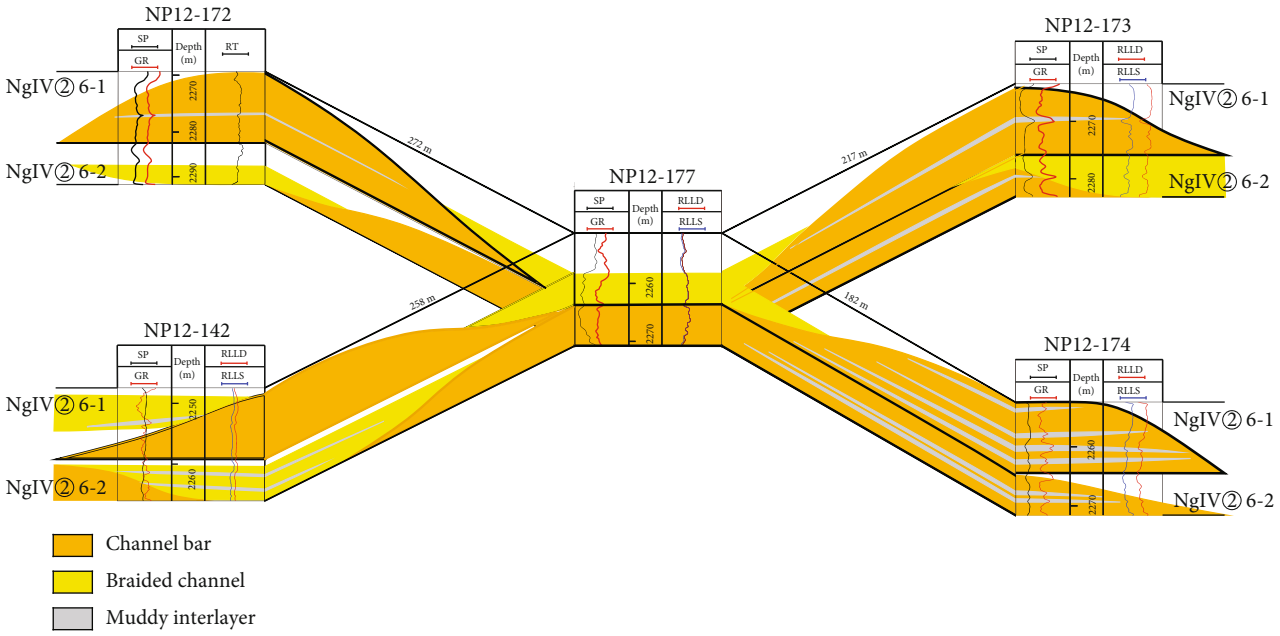

Figure 14: Static distribution model of NP12-177 well group in Nanpu 1-29 Area. Injection well NP12-177, the water injection method is general water injection and the water injection depth of 2258.11-2268.19 m.

was low. However, the area between well NP12-177 and well NP12-174 had many muddy interlayers, which hindered sand connectivity between the two wells.

In addition, based on the dynamic development data including oil production, liquid production, comprehensive water cut of the production wells, and injection volume of injection wells, the dynamic response curve was established (Figure 15). The accuracy of the research on reservoir architecture is verified by comparing the dynamic response curve with the static distribution model [34, 35]. The dynamic response curve selected March 2016 to September 2020 as the evaluation period of dynamic data.

Combined with the dynamic response curve of the NP12-177 well group, it was found that from the beginning of water injection in July 2016 to August 2018, the water injection of well NP12-177 showed a steady upward trend, and the liquid production capacity of the corresponding well NP12-173 maintained a steady increase, and the liquid production capacity of well NP12-174 of the producing well showed a slow downward trend from July 2016 to March 2018. From September 2018 to

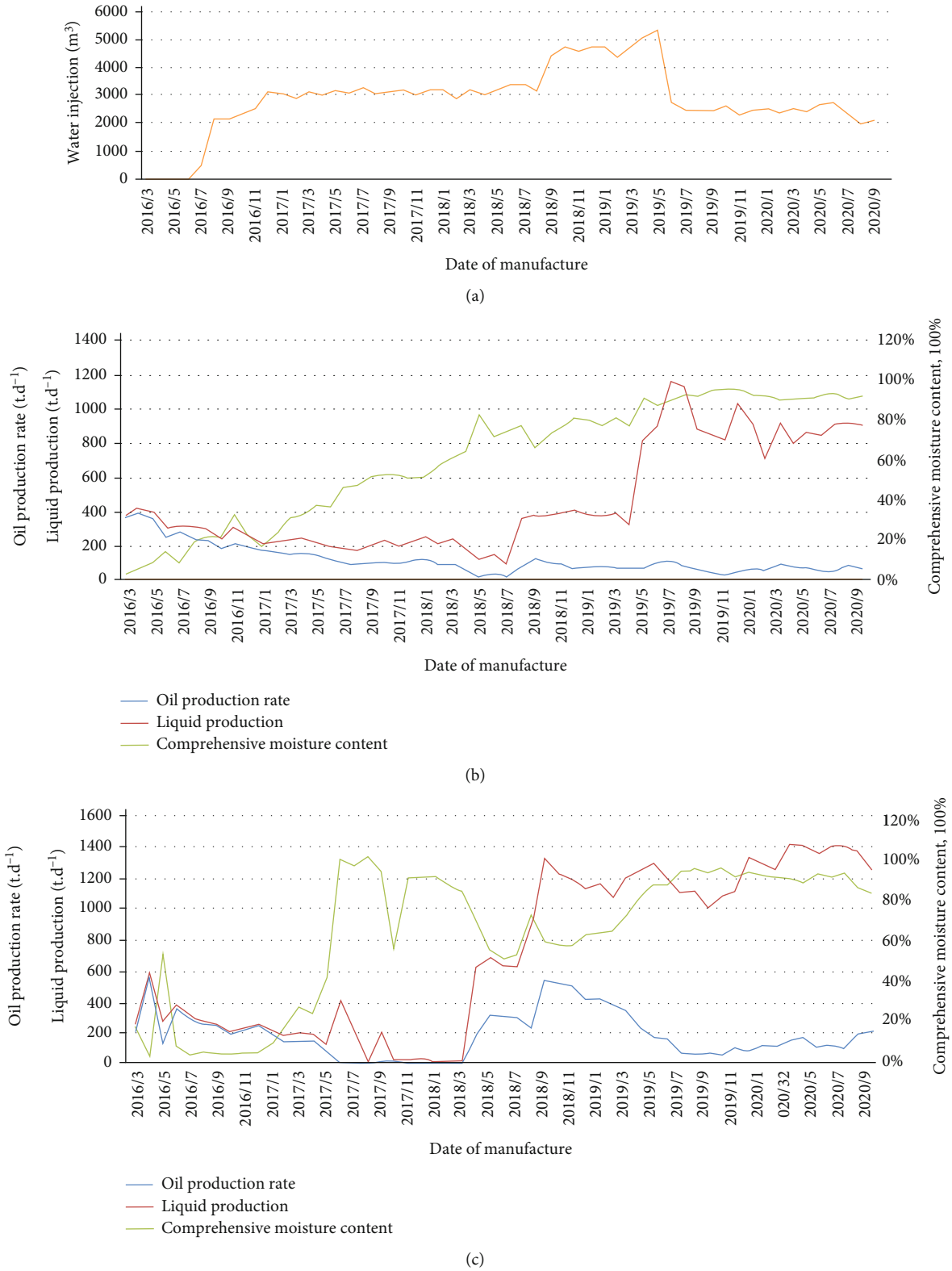

Figure 15: Dynamic response curve of NP12-177 well group in Nanpu 1-29 Area: (a) NP12-177, injection well; (b) NP12-173, production well; (c) NP12-174, production well.

May 2019, the water injection of well NP12-177 in the injection well showed a significant upward trend, and the production capacity of well NP12-173 also realized a substantial increase during this period, while the production capacity of the well NP12-174 showed a steady decline. From June 2019 to September 2020, the water injection capacity of well NP12-177 slowly

declined, but it continued to inject water. At the same time, the fluid production of well NP12-173 also showed a gentle downward trend, while the fluid production of well NP12-174 kept a basic upward trend. Therefore, the study found that the injection volume of well NP12-177 was significantly correlated with the fluctuation range of production capacity of well NP12-173, which was consistent with the good connectivity between well NP12-177 and well NP12-173 in the static distribution model. However, the dynamic response curves of well NP12-177 and well NP12-174 were negatively correlated or irrelevant, which was consistent with the analysis result that the connectivity between well NP12-177 and well NP12-174 was poor due to the development of numerous shale interlayers. Therefore, based on the dynamic development data, the static distribution model and dynamic response curve were compared and analyzed, and it was found that they had good consistency, which confirmed that the above research on reservoir architecture was very correct and reasonable.

7. Conclusions

(1) According to the sedimentary background, granularity characteristics, core characteristics, and sand body distribution characteristics, the braided river type in the study area was determined as wandering braided river

(2) The classification and quantitative architecture characterization in the study area were realized. The architecture classification of the study area was divided into 5-3 levels, including a single braided flow belt, channel bar and braided channel, and interlayer architecture of channel bar

(3) The length of the single braided flow belts was 365.16-1349.72 m, and the width was 270.57-1160.54 m. The channel bar length was distributed 158.89-318.32 m, and the width was 75.97-116.41 m. The braided river width was distributed 16.81-180.05 m. The length and width ratio of the channel bar was concentrated between 2 and 4

(4) Dynamic analysis showed that the research on reservoir architecture was reasonable and accurate. The sand body in the study area was mostly in contact type, so the unevenness of water flooding degree should be paid attention to in the remaining oil development process, to guide the later oilfield development and adjustment

Data Availability

The data used to support the findings of this study are available from the corresponding authors.

Conflicts of Interest

The authors declare that they have no conflicts of interest.

Acknowledgments

This study was financially supported by the National Natural Science Foundation of China (Grant Nos. 42130813 and 41872138).

References

[1] J. R. L. Allen, "Studies in fluviatile sedimentation: bars, bar-complexes and sandstone sheets (low-sinuosity braided streams) in the brownstones (L. devonian), welsh borders," *Sedimentary Geology*, vol. 33, no. 4, pp. 237–293, 1983.

[2] A. D. Miall, "Architectural-element analysis: a new method of facies analysis applied to fluvial deposits," *Earth-Science Reviews*, vol. 22, no. 4, pp. 261–308, 1985.

[3] A. D. Miall, *The Geology of Fluvial Deposits: Sedimentary Facies, Basin Analysis, and Petroleum Geology*, Spring, Berlin, 2013.

[4] J. S. Bridge and R. S. Tye, "Interpreting the dimensions of ancient fluvial channel bars, channels, and channel belts from wireline-logs and cores," *AAPG Bulletin*, vol. 84, no. 8, pp. 1205–1228, 2000.

[5] R. L. Skelly, C. S. Bristow, F. G. Ethridge et al., "Architecture of channel-belt deposits in an aggrading shallow sandbed braided river: the lower Niobrara River, northeast Nebraska," *Sedimentary Geology*, vol. 158, no. 3-4, pp. 249–270, 2003.

[6] M. U. Longxin and Z. H. A. O. Guoliang, "Architecture analysis of reservoirs in branching- and wandering-based braided rivers: taking FN field, Sudan as an example," *Earth Science Frontiers*, vol. 24, no. 2, pp. 246–256, 2017.

[7] D. Yue, W. Li, J. Li et al., "Variable architecture models of fluvial reservoir controlled by base-level cycle - a case study of Jurassic outcrop in Datong Basin," *Earth Science*, vol. 42, no. - article 20220418, 2022.

[8] W. Wu, Q. Li, J. Yu, C. Lin, D. Li, and T. Yang, "The Central Canyon depositional patterns and filling process in east of Lingshui Depression, Qiongdongnan Basin, northern South China Sea," *Geological Journal*, vol. 53, no. 6, pp. 3064–3081, 2018.

[9] Q. Li, W. Wu, J. Liang et al., "Deep-water channels in the lower Congo basin: evolution of the geomorphology and depositional environment during the Miocene," *Marine and Petroleum Geology*, vol. 115, article 104260, 2020.

[10] Y. Dali, *The Study on Architecture Analysis and Remaining Oil Distribution Patterns of Meandering River Reservoir: A case study of Guantao Formation, Gudao Oilfield*, China University of Petroleum(Beijing), 2006.

[11] X. Wang, Y. Liu, J. Hou et al., "The relationship between syn-sedimentary fault activity and reservoir quality—a case study of the Ek1 formation in the Wang Guantun area, China," *Interpretation*, vol. 8, no. 3, p. SM15, 2020.

[12] X. Wang, X. Zhou, S. Li, N. Zhang, L. Ji, and H. Lu, "Mechanism study of hydrocarbon differential distribution controlled by the activity of growing faults in faulted basins: case study of Paleogene in the Wang Guantun area," *Lithosphere*, vol. 2021, p. 7115985, 2022.

[13] H. Zhang, M. Li, Y. Kang, Z. Wu, and G. Wang, "Reservoir architecture and fine characterization of remaining oil of Chang 3 reservoir in Zhenbei oilfield, Ordos Basin," *Lithologic Reservoirs*, vol. 33, no. 6, pp. 1–12, 2021.

[14] Z. Lin, H. Wang, H. Jiang et al., "Volcanic events at the stage of Guantao Formation in Nanpu San and its petroleum geological significance," *Marine Geology & Quaternary Geology*, vol. 31, no. 3, pp. 79–85, 2011.

[15] C. G. Liang, "Sedmentary microfacies of the Q4 member of cretaceous in Fuyu Oilfield, Songliao basin," *Journal of Southwest Petroleum University (Science & Technology Edition)*, vol. 30, no. 2, pp. 69–73, 2008.

[16] L. Baofang, Z. Weimin, L. Lie et al., "Study on modern deposit of a braided stream and facies model: taking the Yongding River as an example," *Acta Sedimentologica Sinica*, vol. 16, no. 1, p. 34, 1998.

[17] H. Liu, C. Y. Lin, and X. G. Zhang, "Reservoir architecture and remaing oil distribution in braided river of Guantao Formation, Kongdian oilfield," *Journal of Jilian University (Earth Science Edition)*, vol. 48, no. 3, pp. 665–677, 2018.

[18] J. Yuanpeng, Z. Lan, Z. Guangyi et al., "Lobate shallow-water delta reservoir architecture characterization in the southern Bohai Sea," *Special Oil & Gas Reservoirs*, vol. 27, no. 6, pp. 88–95, 2020.

[19] X. Wang, S. Yu, S. Li, and N. Zhang, "Two parameter optimization methods of multi-point geostatistics," *Journal of Petroleum Science & Engineering*, vol. 208, p. 109724, 2022.

[20] X. Wang, J. Hou, S. Li et al., "Insight into the nanoscale pore structure of organic-rich shales in the Bakken Formation, USA," *Journal of Petroleum Science & Engineering*, vol. 191, p. 107182, 2020.

[21] G. Qin, S. Wu, and X. Song, "Sedimentary characteristics of distal fine-grain delta and architecture analysis of single sand body," *Journal of China University of Petroleum (Edition of Nature Science)*, vol. 41, no. 6, pp. 9–19, 2017.

[22] X. J. Wu, H. B. Su, S. J. Zhang, L. J. Feng, J. Wang, and S. L. Jie, "Architecture anatomy and hierachical modeling of sand-gravel braided river reservoirs: a case study of Zhong32 wells area, Qigu Formation reservoir, Fengceng oilfield," *Acta Sedimentologica Sinica*, vol. 38, no. 5, pp. 933–945, 2020.

[23] J. Li, C. Huo, X. Ye, P. Wang, J. Xu, and J. Yang, "Internal architecture characteristics of sandy braided-river reservoirs in L Oilfield, Bohai Bay Basin," *Petroleum Geology and Recovery Efficiency*, vol. 24, no. 6, pp. 48–53, 2017.

[24] S. F. Leclair and J. S. Bridge, "Quantitative interpretation of sedimentary structures formed by river dunes," *Journal of Sedimentary Research*, vol. 71, no. 5, pp. 713–716, 2001.

[25] L. Shunming, S. Xinmin, J. Youwei, L. Lang, C. Nengxue, and S. Jingmin, "Architecture and remaining oil distribution of the sandy braided river reservoir in the Gaoshangpu Oilfield," *Petroleum Exploration and Development*, vol. 38, no. 4, pp. 474–482, 2011.

[26] D. Q. Xu, Z. X. Sun, Y. F. Ren, and C. Yang, "Geological modeling of braided river tight reservoir based on geological knowledge database," *Fault-Block Oil & Gas Field*, vol. 25, no. 1, pp. 57–61, 2018.

[27] L. Huang, W. He, P. Tao, J. Li, X. Wang, and X. Wang, "Reservoir architecture and remaining oil enrichment pattern of braided river——a case study from Huanjiang oilfield in Ordos Basin," *Petroleum Geology and Engineering*, vol. 31, no. 1, pp. 96–103, 2017.

[28] H. Zhao, X. W. Yang, W. C. Yue et al., "Sedimentary facies characteristics and sandbody superimposition relation of Yan'an Formation in Jing'an area," *Journal of Xi'an University of Science and Technology*, vol. 40, no. 4, pp. 646–657, 2020.

[29] Y. Guo, Z. Cai, F. Yu, X. Zhang, and B. Li, "Sandbody superimposition relation of 8th member of Shihezi Formation in southeastern Sulige and its influence on gas-water distribution," *Journal of Xi'an Shiyou University (Natural Science Edition)*, vol. 33, no. 4, pp. 1–7, 2018.

[30] C. J. Feng, Z. D. Bao, C. M. Dai, and Z. Q. Zhang, "Superimposition patterns of underwater distributary channel sands in deltaic front and its control in remaining oil distribution: a case study from K_1q^4 in J19 block, Fuyu oilfield," *Oil & Gas Geology*, vol. 36, no. 1, pp. 128–135, 2015.

[31] X. Wang, F. Zhang, S. Li et al., "The architectural surfaces characteristics of sandy braided river reservoirs, case study in Gudong Oil Field, China," *Geofluids*, Article ID 8821711, 2021.

[32] Y. Gao, Y. Yin, P. Pan, S. Yu, and Y. Gu, "The effects of incline heterolithic strata on SAGD development," *Oil Drilling & Production Technology*, vol. 42, no. 6, pp. 767–771, 2020.

[33] L. Xuyan, *Study on the Method of the Spatial Locating of Macroscopic Throats and the Potential Technology in HYJZ9-3 Oilfield*, China University of Petroleum, 2019.

[34] L. Xu, S. Li, X. Yu, T. Zhang, X. Luo, and G. Jiang, "Analysis of reservoir architecture in the braided river delta front: a case study of the Sangonghe Formation in Block Cai9 of Cainan oilfield," *Petroleum Geology and Recovery Efficiency*, vol. 23, no. 5, pp. 50–57, 2016.

[35] C. Lyu, X. Wang, X. Lu et al., "Evaluation of hydrocarbon generation using struc-tural and thermal modeling in the thrust belt of Kuqa Foreland Basin, NW China," *Geofluids*, vol. 2020, Article ID 8894030, 18 pages, 2020.